

1 **Embryonic origin of the gnathostome vertebral skeleton**

2

3 Katharine E. Criswell^{1,2,3*}, Michael I. Coates², and J. Andrew Gillis^{1,3}

4

5 Affiliations:

6 ¹Department of Organismal Biology and Anatomy, University of Chicago, Chicago, IL

7 ²Department of Zoology, University of Cambridge, Cambridge, UK

8 ³Marine Biological Laboratory, Woods Hole, MA

9

10 *Correspondence to kc518@cam.ac.uk

11

12

13

14

15

16

17

18

19

20

21

22

23

24

25

26 Abstract

27 The vertebral column is a key component of the jawed vertebrate (gnathostome) body plan,
28 but the primitive embryonic origin of this skeleton remains unclear. In tetrapods, all vertebral
29 components (neural arches, haemal arches, and centra) derive from paraxial mesoderm
30 (somites). However, in teleost fishes, vertebrae have a dual embryonic origin, with arches
31 derived from somites, but centra formed, in part, by secretion of bone matrix from the
32 notochord. Here, we test the embryonic origin of the vertebral skeleton in a cartilaginous fish
33 (the skate, *Leucoraja erinacea*) which serves as an outgroup to tetrapods and teleosts. We
34 demonstrate, by cell lineage tracing, that both arches and centra are somite-derived. We find
35 no evidence of cellular or matrix contribution from the notochord to the skate vertebral
36 skeleton. These findings indicate that the earliest gnathostome vertebral skeleton was
37 exclusively of somitic origin, with a notochord contribution arising secondarily in teleosts.

38

39 Key Words

40 Vertebral skeleton, skate, somite, notochord, vertebrae, evolution

41

42 Introduction

43 The presence of vertebrae is a defining feature of the vertebrate body plan. A
44 vertebral skeleton may consist of a series of paired neural arches that cover the spinal cord,
45 paired haemal arches that enclose the caudal artery and vein, and, in many jawed vertebrates
46 (gnathostomes), a series of centra that replace the notochord as the predominant support
47 structure. Vertebral centra are highly variable in terms of morphology and tissue
48 composition, and likely evolved independently in many different gnathostome lineages,
49 including tetrapods, teleost fishes, and cartilaginous fishes [1]. This apparent evolutionary

50 convergence raises questions about the embryonic origin of vertebral skeletal elements across
51 gnathostomes.

52 In tetrapods, all components of the vertebral skeleton derive from somites: transient,
53 bilateral blocks of segmented paraxial mesoderm that form dorsally within the embryonic
54 trunk. Somites are subdivided into dorsal and ventral subpopulations that give rise to trunk
55 connective tissue and musculature (“dermomyotome”) and skeletal tissues (“sclerotome”),
56 respectively. Cell lineage tracing experiments using chick-quail chimaeras [2–5] and
57 fluorescein-dextran injections or grafts from GFP-transgenic donor embryos in axolotl [6]
58 have shown a fully somitic origin of the vertebral skeleton in these taxa, with somite-derived
59 cells recovered in developing arches and nascent cartilage of the centra.

60 Conversely, in teleost ray-finned fishes, the vertebral skeleton appears to have a dual
61 embryonic origin, with contributions from both paraxial mesoderm and the notochord.
62 Teleost vertebral centra consist of an inner layer (the chordacentrum) and an outer layer, both
63 composed of bone that forms by intramembranous ossification [7]. The chordacentrum of
64 teleosts forms first, by secretion of bone matrix proteins (e.g. SPARC, type I collagen) from
65 “chordoblast” cells that reside within the notochord epithelium [8–10]. In zebrafish, *in vitro*
66 assays have shown that cultured notochord cells have the capacity to secrete bone matrix, and
67 ablation experiments have demonstrated that in the absence of notochord, chordacentra fail to
68 form [11]. Teleost chordacentra are subsequently surrounded by a relatively late-developing
69 layer of paraxial mesoderm-derived membrane bone [7,12]. Additionally, zebrafish mutants
70 with somite patterning defects possess normally-developing chordacentra, but exhibit
71 profound neural and haemal arch defects, indicating the likely paraxial mesodermal origin of
72 arch tissues [11,13,14].

73 To determine whether the dual origin of vertebral centra is a teleost-specific feature of
74 the vertebral skeleton, or a general feature for gnathostomes that has been lost in tetrapods,

75 data on the embryonic origin of vertebrae from an outgroup to the bony fishes (i.e.
76 Osteichthyes: the group that includes tetrapods and teleosts) are needed. Cartilaginous fishes
77 (Chondrichthyes: sharks, skates, rays and holocephalans) occupy a key phylogenetic position
78 as the sister group to the bony fishes, and data from this lineage may therefore be used to
79 help infer primitive developmental conditions for the last common ancestor of gnathostomes.
80 We have previously shown that vertebrae in the little skate (*Leucoraja erinacea*) each consist
81 of a dorsal neural spine, two sets of dorsal cartilages that enclose the spinal cord (neural and
82 intercalary arches), a single haemal arch and spine extending ventrally, and a tri-layered
83 centrum (Figure 1) [15]. Here, we use somite and notochord fate mapping experiments, as
84 well as mRNA *in situ* hybridization for genes encoding skeletal matrix proteins, to test the
85 embryonic origin of the skate vertebral skeleton. We show that all components of the skate
86 vertebral skeleton derive from paraxial mesoderm, with no evidence for cellular or matrix
87 contributions from the notochord. When considered alongside data from bony fishes, our
88 findings point to a general and likely primitive paraxial mesodermal origin of the vertebrate
89 column in jawed vertebrates.

90

91 **Materials and Methods**

92 *Somite fate mapping*

93 *L. erinacea* embryos were obtained from the Marine Biological Laboratory (MBL) in Woods
94 Hole, MA and kept in a flow-through sea table at ~16°C until S24. A flap was cut in the egg
95 case using a razor blade, and the embryo and yolk were transferred to a Petri dish. Embryos
96 were anesthetized in a solution of MS-222 (100mg/L Ethyl 3-aminobenzoate
97 methanesulfonate – Sigma-Aldrich) in seawater. CellTracker CM-DiI (Thermofisher) (5
98 µg/µL in ethanol) was diluted 1:10 in 0.3 M sucrose and injected into the ventral portions of
99 the somites (1-3 injections per embryo) using a pulled glass capillary needle and a

100 Picospritzer pressure injector (Figure 2a). Embryos were then replaced in their egg cases and
101 returned to the sea table to develop for approximately 7 or 12 weeks. Embryos were then
102 fixed with 4% PFA, as described in Criswell et al. [15].

103

104 *Notochord fate mapping*

105 Embryos were kept as described above until S14, at which point a small window was
106 cut in the egg case over the embryo. CM-DiI was microinjected into the notochord triangle as
107 described above (Figure 2b). The window was then sealed with donor eggshell and Krazy
108 Glue™ gel (Figure 2c), and eggs were returned to the sea table to develop for an additional
109 16-18 weeks prior to fixation (as described in Criswell et al. [15]).

110

111 *Validation of CM-DiI injection placement*

112 To verify the correct placement of CM-DiI injections, three somite-injected embryos
113 were fixed immediately post-injection, and three notochord-injected embryos were fixed five
114 days post-injection. Embryos were fixed in 4% paraformaldehyde in PBS overnight at 4°C,
115 rinsed 3X15 min in PBS, and stained with DAPI at 1µg/mL overnight at room temperature.
116 Somite-injected embryos were imaged on a Zeiss lightsheet microscope and notochord-
117 injected embryos were imaged on Zeiss lightsheet or LSM 780 confocal microscopes.

118

119 *Histology and mRNA in situ hybridization*

120 CM-DiI-labeled *L. erinacea* embryos were embedded in paraffin wax and sectioned at
121 8 µm thickness as described in O'Neill et al. [16] for histological analysis. Prior to
122 embedding, embryos were demineralized in 10% EDTA (ethylenediaminetetraacetic acid) for
123 14 days. Histochemical staining was performed following the Masson's trichrome protocol of
124 Witten and Hall [17]. *In situ* hybridization experiments for *Coll1a1* (GenBank accession

125 number MG017616) and *SPARC* (GenBank accession number MG017615) were performed
126 on sections as described in O'Neill et al. [16], with modifications according to Gillis et al.
127 [18].

128 **Results**

129 *Somitic contribution to all components of the skate vertebral skeleton*

130 To test for somitic contribution to the skate vertebral skeleton, we microinjected CM-
131 DiI into ventral portions of the somites (i.e. the presumptive sclerotome – Figure 3a) of skate
132 embryos at stage (S) 24 (Ballard et al., 1993). Focal labeling of the somites (with no
133 notochordal contamination) was confirmed by light sheet microscopy, in embryos fixed
134 immediately post-injection (Figure 3b; n=3). By 50-52 days post-injection (dpi) (S31),
135 spindle-shaped cells of the developing areolar tissue of the centrum surround the notochord,
136 and preskeletal mesenchyme has condensed around the neural tube and caudal artery and
137 vein. In all embryos analyzed at this stage (n=5), CM-DiI was recovered in the spindle-
138 shaped cells of the developing areolar tissue (Figure 3c), indicating their somitic origin.

139 By 109dpi (S34), vertebrae are fully developed, with neural, intercalary and haemal
140 arches, and a tri-layered centrum (Figure 1). In embryos analyzed at this stage (n=4), CM-
141 DiI-positive cells were recovered throughout the vertebral skeleton. CM-DiI-positive cells
142 were recovered in the cartilage of the neural (n=3 vertebrae in three embryos) and haemal
143 arches (n=6 vertebrae in four embryos; Figure 3d, e), as well as in the inner layer of cartilage
144 (Figure 3f; n=2 vertebrae in two embryos), the middle areolar tissue (Figure 3g; n=3
145 vertebrae in three embryos), and the outer cartilage of the centrum (Figure 3h; n=3 vertebrae
146 in three embryos). Taken together, these findings demonstrate somitic contribution to all
147 major components of the skate vertebral skeleton.

148

149 *No evidence for notochordal contribution to the vertebral skeleton in skate*

150 To test for cellular contributions of the notochord to the skate vertebral skeleton, we
151 conducted a series of notochord fate mapping experiments. In cartilaginous fishes, the
152 notochord derives from a small triangular region of progenitor cells (the “notochord
153 triangle”) that appears at the posterior margin of the blastodisc at S12 [19]. We focally
154 labeled the notochord triangle of skate embryos with CM-DiI at S14 (Figure 4a), and we
155 confirmed localization of the dye to the notochord at 5dpi (approximately S17) using
156 confocal microscopy. In three embryos examined at S17, CM-DiI was found either only in
157 the notochord (n=2), or in the notochord and neural tissue (n=1) (Figure 4b). In no cases were
158 CM-DiI-labeled cells detected in the paraxial mesoderm.

159 We therefore labeled the notochord triangles of several skate embryos at S14, and
160 reared these embryos to 116-129dpi (S34 – at which point the vertebral skeleton has fully
161 differentiated). CM-DiI was recovered within the notochord (Figure 4c, c’) and the notochord
162 epithelium (Figure 4d, d’) of the intervertebral regions of the axial column (n=5). In three
163 embryos, CM-DiI-positive cells were recovered in the remnants of notochord epithelium that
164 persist in the center of the centrum, where the notochord is almost completely replaced by
165 inner layer centrum cartilage, but no CM-DiI-positive chondrocytes were recovered in the
166 inner layer of cartilage itself. No CM-DiI labeled chondrocytes were observed in any other
167 components of the axial column. These experiments, therefore, provide no evidence for a
168 cellular contribution from the notochord to the vertebral skeleton.

169 In teleosts, chordoblast cells within the notochord epithelium secrete matrix
170 components that make up the acellular bone of the chordacentrum. Though skates do not
171 possess a chordacentrum, the areolar tissue of the skate centrum does mineralize, and at its
172 origin, sits adjacent to the notochord epithelium [15]. To test whether notochord epithelial
173 cells contribute matrix components to centrum tissue in skate, we characterised the
174 expression of genes encoding the bone matrix proteins *Col1a1* and *SPARC* in developing

175 skate centra. We did not detect transcription of *Colla1* (Figure 5a) or *SPARC* (Figure 5b) in
176 the notochord epithelium. Rather, these transcripts localized to the spindle-shaped cells of the
177 areolar tissue (Figure 5a-b). These findings suggest that the paraxial mesoderm-derived cells
178 of the areolar tissue itself – and not the notochord epithelium – are the source of extracellular
179 matrix of the mineralized tissue of the skate vertebral centrum.

180

181 **Discussion**

182 Our somite fate mapping experiments demonstrate that presumptive sclerotome
183 contributes to all components of the vertebrae in skate, including the neural and haemal
184 arches, and all tissues of the tri-layered vertebral centrum. While it is possible that DiI could
185 diffuse through the extracellular matrix after injection to contaminate tissues adjacent to the
186 intended target (e.g. notochord), we have controlled for this possibility by imaging a subset
187 of embryos shortly after injection to validate the precision of our labeling, and by performing
188 complementary notochord fate mapping experiments. In the latter, we find that CM-DiI
189 labeling of notochord progenitor cells resulted exclusively in labeling of the notochord and
190 the notochord epithelium, with no contribution to vertebral tissues. In teleost fishes,
191 chordoblast cells within the notochord epithelium express genes encoding the bone matrix
192 proteins type I collagen and SPARC [10,20–22], and are likely the source of bone matrix for
193 the earliest layer of the vertebral centrum [11,23–28]. As skates also possess a mineralized
194 layer within their vertebral centra, we sought to test for expression of *Colla1* and *SPARC*
195 during skate vertebral development by mRNA *in situ* hybridization. We found these genes to
196 be expressed exclusively within the somitically-derived spindle-shaped cells of the areolar
197 tissue (the precursor to the mineralized middle layer of the centrum – Criswell et al. [15]),
198 and not in the notochord epithelium. These findings suggest that the cells and matrix
199 components of the skate vertebral centrum are entirely of paraxial mesodermal origin.

200 When considered alongside data from bony fishes, our demonstration of a somitic
201 origin of the vertebral skeleton of skates suggests that this tissue was likely the sole, primitive
202 source of vertebral skeletal tissues in gnathostomes, with a notochord contribution to centrum
203 bone representing a derived condition of teleost fishes (Figure 6). Evidence from early fossil
204 jawed and jawless fishes strongly suggests that the vertebral skeleton in the last common
205 ancestor of gnathostomes consisted simply of a series of neural arches and a persistent
206 notochord, with no centra [29–32]. Several gnathostome lineages, including elasmobranch
207 cartilaginous fishes, teleosts, and tetrapods, subsequently evolved centra independently of
208 one another [1]. At their origins, the vertebral centra of elasmobranchs and tetrapods derived
209 entirely from paraxial mesoderm [3,6,12], but an inner layer of notochord-derived acellular
210 bone was incorporated into the centrum with the independent origin of teleost centra.

211 It is not yet clear, however, if this specialized condition of teleosts is unique among
212 ray-finned fishes. Despite recent changes to phylogenetic patterns [33] vertebral centra very
213 likely evolved independently in multiple non-teleost ray-finned fish lineages (e.g. in gars and
214 bichirs [1,34,35]. But, it is unclear whether the notochord contributes tissue to the different
215 forms of centra observed in these taxa. Comprehensive analyses of the embryonic origins of
216 vertebral tissues in strategically selected fish taxa are needed to better resolve the
217 evolutionary and developmental assembly of the diverse array of axial skeletons, arguably
218 the key characteristic, of vertebrates in general.

219

220 **Ethics**

221 All experimental work was done in compliance with protocols approved by the Animal Care
222 and Use Committee at the Marine Biological Laboratory.

223

224 **Data Accessibility**

225 The sequence data associated with the genes in this study are available on GenBank (*Colla1*
226 accession number MG017616 and *SPARC* accession number MG017615).

227

228 **Competing Interests**

229 The authors declare no competing interests.

230

231 **Author Contributions**

232 KEC conceived of the study, performed histology, fate mapping, and *in situ*
233 hybridization experiments, and drafted the manuscript; MIC coordinated the study and
234 provided input on the manuscript; JAG designed portions of the study, coordinated the study,
235 and helped to write the manuscript. All authors gave final approval for publication.

236

237 **Acknowledgements**

238 We thank H. Stinnett, R. Ho, M. Hale, A. Fleming, and M. Kishida for helpful
239 discussions. We also acknowledge the support of R. Behringer, A. Sánchez-Alvarado, J.
240 Henry, D. Lyons, the MBL Embryology community, and the staff of the MBL Marine
241 Resources Center.

242

243 **References**

- 244 1. Arratia G, Schultze H-P, Casciotta J. 2001 Vertebral column and associated elements in
245 dipnoans and comparison with other fishes: development and homology. *J. Morphol.*
246 **250**, 101–172.
- 247 2. Stern CD, Keynes RJ. 1987 Interactions between somite cells: the formation and
248 maintenance of segment boundaries in the chick embryo. *Development* **99**, 261–272.
- 249 3. Bagnall KM, Higgins SJ, Sanders EJ. 1988 The contribution made by a single somite to
250 the vertebral column: experimental evidence in support of resegmentation using the
251 chick-quail chimaera model. *Development* **103**, 69–85.

- 252 4. Aoyama H, Asamoto K. 2000 The developmental fate of the rostral/caudal half of a
253 somite for vertebra and rib formation: experimental confirmation of the resegmentation
254 theory using chick-quail chimeras. *Mech. Dev.* **99**, 71–82. (doi:10.1016/S0925-
255 4773(00)00481-0)
- 256 5. Christ B, Huang R, Scaal M. 2004 Formation and differentiation of the avian sclerotome.
257 *Anat. Embryol. (Berl.)* **208**, 333–350. (doi:10.1007/s00429-004-0408-z)
- 258 6. Piekarski N, Olsson L. 2014 Resegmentation in the mexican axolotl, *Ambystoma*
259 *mexicanum*. *J. Morphol.* **275**, 141–152. (doi:10.1002/jmor.20204)
- 260 7. Bensimon-Brito A, Cardeira J, Cancela ML, Huysseune A, Witten PE. 2012 Distinct
261 patterns of notochord mineralization in zebrafish coincide with the localization of
262 Osteocalcin isoform 1 during early vertebral centra formation. *BMC Dev. Biol.* **12**, 28.
263 (doi:10.1186/1471-213X-12-28)
- 264 8. Grotmol S, Nordvik K, Kryvi H, Totland GK. 2005 A segmental pattern of alkaline
265 phosphatase activity within the notochord coincides with the initial formation of the
266 vertebral bodies. *J. Anat.* **206**, 427–436.
- 267 9. Renn J, Schaedel M, Volff J-N, Goerlich R, Scharl M, Winkler C. 2006 Dynamic
268 expression of *sparc* precedes formation of skeletal elements in the Medaka (*Oryzias*
269 *latipes*). *Gene* **372**, 208–218. (doi:10.1016/j.gene.2006.01.011)
- 270 10. Kaneko T, Freeha K, Wu X, Mogi M, Uji S, Yokoi H, Suzuki T. 2016 Role of notochord
271 cells and sclerotome-derived cells in vertebral column development in fugu, *Takifugu*
272 *rubripes*: histological and gene expression analyses. *Cell Tissue Res.* **366**, 37–49.
273 (doi:10.1007/s00441-016-2404-z)
- 274 11. Fleming A, Keynes R, Tannahill D. 2004 A central role for the notochord in vertebral
275 patterning. *Development* **131**, 873–880. (doi:10.1242/dev.00952)
- 276 12. Morin-Kensicki EM, Melancon E, Eisen JS. 2002 Segmental relationship between
277 somites and vertebral column in zebrafish. *Development* **129**, 3851–3860.
- 278 13. Eeden FJ van *et al.* 1996 Mutations affecting somite formation and patterning in the
279 zebrafish, *Danio rerio*. *Development* **123**, 153–164.
- 280 14. Fleming A, Keynes RJ, Tannahill D. 2001 The role of the notochord in vertebral column
281 formation. *J. Anat.* **199**, 177–180. (doi:10.1017/S0021878201008044)
- 282 15. Criswell KE, Coates MI, Gillis JA. 2017 Embryonic development of the axial column in
283 the little skate, *Leucoraja erinacea*. *J. Morphol.* **278**, 300–320. (doi:10.1002/jmor.20637)
- 284 16. O’Neill P, McCole RB, Baker CVH. 2007 A molecular analysis of neurogenic placode
285 and cranial sensory ganglion development in the shark, *Scyliorhinus canicula*. *Dev. Biol.*
286 **304**, 156–181. (doi:10.1016/j.ydbio.2006.12.029)
- 287 17. Witten PE, Hall BK. 2003 Seasonal changes in the lower jaw skeleton in male Atlantic
288 salmon (*Salmo salar* L.): remodelling and regression of the kype after spawning. *J. Anat.*
289 **203**, 435–450. (doi:10.1046/j.1469-7580.2003.00239.x)

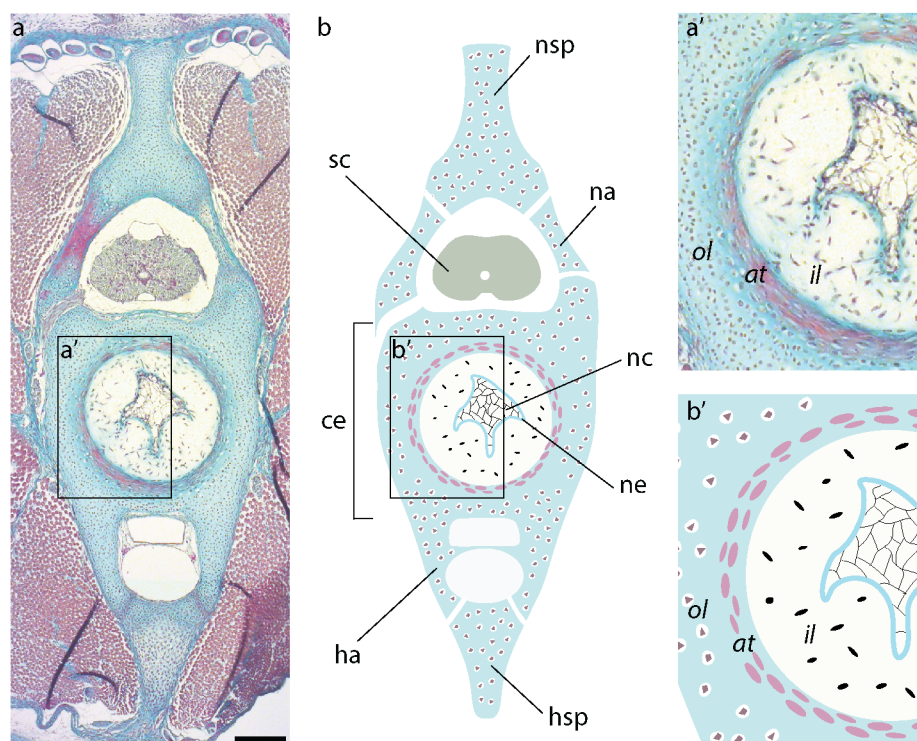
- 290 18. Gillis JA, Modrell MS, Northcutt RG, Catania KC, Luer CA, Baker CVH. 2012
 291 Electrosensory ampullary organs are derived from lateral line placodes in cartilaginous
 292 fishes. *Development* **139**, 3142–3146. (doi:10.1242/dev.084046)
- 293 19. Ballard WW, Mellinger J, Lechenault H. 1993 A series of normal stages for development
 294 of *Scyliorhinus canicula*, the lesser spotted dogfish (Chondrichthyes:Scyliorhinidae). *J.*
 295 *Exp. Zool.* **267**, 318–336.
- 296 20. Thisse B *et al.* 2001 Expression of the zebrafish genome during embryogenesis (NIH
 297 R01 RR15402). *Zfin Direct Data Submiss.*
- 298 21. Rotllant J, Liu D, Yan Y-L, Postlethwait JH, Westerfield M, Du S-J. 2008 Sparc
 299 (Osteonectin) functions in morphogenesis of the pharyngeal skeleton and inner ear.
 300 *Matrix Biol.* **27**, 561–572. (doi:10.1016/j.matbio.2008.03.001)
- 301 22. Wang S, Furmanek T, Kryvi H, Krossøy C, Totland GK, Grotmol S, Wargelius A. 2014
 302 Transcriptome sequencing of Atlantic salmon (*Salmo salar* L.) notochord prior to
 303 development of the vertebrae provides clues to regulation of positional fate, chordoblast
 304 lineage and mineralisation. *BMC Genomics* **15**, 141. (doi:10.1186/1471-2164-15-141)
- 305 23. Ramanujam SG. 1929 The study of the development of the vertebral column in teleosts,
 306 as shown in the life-history of the herring. *J. Zool.* **99**, 365–414.
- 307 24. Mookerjee HK, Mitra GN, Mazumdar SR. 1940 The development of the vertebral
 308 column of a viviparous teleost, *Lebistes reticulatus*. *J. Morphol.* **67**, 241–269.
 309 (doi:10.1002/jmor.1050670203)
- 310 25. Laerm J. 1976 The development, function, and design of amphicoelous vertebrae in
 311 teleost fishes. *Zool. J. Linn. Soc.* **58**, 237–254.
- 312 26. Grotmol S, Kryvi H, Nordvik K, Totland GK. 2003 Notochord segmentation may lay
 313 down the pathway for the development of the vertebral bodies in the Atlantic salmon.
 314 *Anat. Embryol. (Berl.)* **207**, 263–272. (doi:10.1007/s00429-003-0349-y)
- 315 27. Nordvik K, Kryvi H, Totland GK, Grotmol S. 2005 The salmon vertebral body develops
 316 through mineralization of two preformed tissues that are encompassed by two layers of
 317 bone. *J. Anat.* **206**, 103–114. (doi:10.1111/j.1469-7580.2005.00372.x)
- 318 28. Renn J, Büttner A, To TT, Chan SJH, Winkler C. 2013 A col10a1:nlGFP transgenic line
 319 displays putative osteoblast precursors at the medaka notochordal sheath prior to
 320 mineralization. *Dev. Biol.* **381**, 134–143. (doi:10.1016/j.ydbio.2013.05.030)
- 321 29. Gardiner BG, Miles RS. 1994 Eubrachythoracid arthrodires from gogo, western australia.
 322 *Zool. J. Linn. Soc.* **112**, 443–477.
- 323 30. Janvier P. 1996 *Early Vertebrates*. Oxford: Clarendon Press.
- 324 31. Long JA, Trinajstić K, Young GC, Senden T. 2008 Live birth in the Devonian period.
 325 *Nature* **453**, 650–652. (doi:10.1038/nature06966)

- 326 32. Johanson Z, Trinajstic K, Carr R, Ritchie A. 2013 Evolution and development of the
 327 synarcual in early vertebrates. *Zoomorphology* **132**, 95–110. (doi:10.1007/s00435-012-
 328 0169-9)
- 329 33. Giles S, Xu G-H, Near TJ, Friedman M. 2017 Early members of ‘living fossil’ lineage
 330 imply later origin of modern ray-finned fishes. *Nature* **549**, 265–268.
 331 (doi:10.1038/nature23654)
- 332 34. Laerm J. 1979 The origin and homology of the chondrosteian vertebral centrum. *Can. J.*
 333 *Zool.* **57**, 475–485.
- 334 35. Laerm J. 1982 The origin and homology of the neopterygian vertebral centrum. *Journal*
 335 *of Paleontology* **56**, 191–202.
- 336 36. Goodrich E. 1930 *Studies on the Structure and Development of Vertebrates*. London:
 337 Dover Publications.
- 338 37. MacBride EW. 1932 Recent work on the development of the vertebral column. *Biol Rev*
 339 **7**, 108–148.

340

341 **Figures**

342

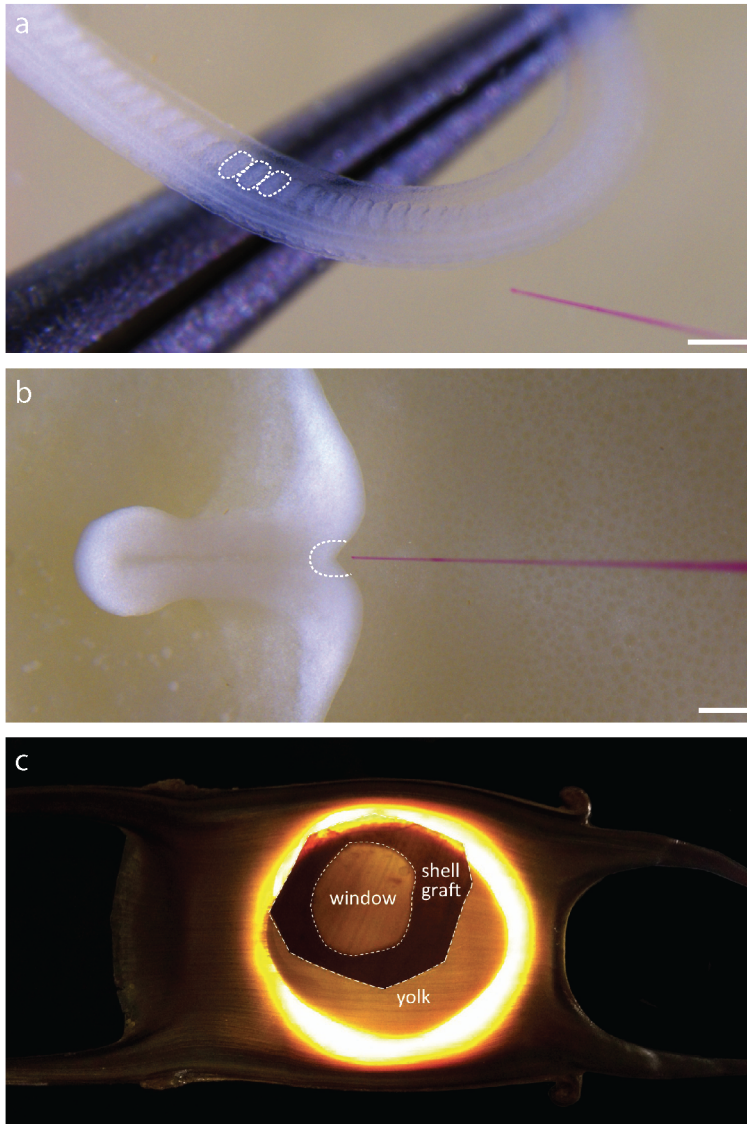


343

344 **Figure 1.** a, Cross section through a skate caudal vertebra (stained with Masson's trichrome);

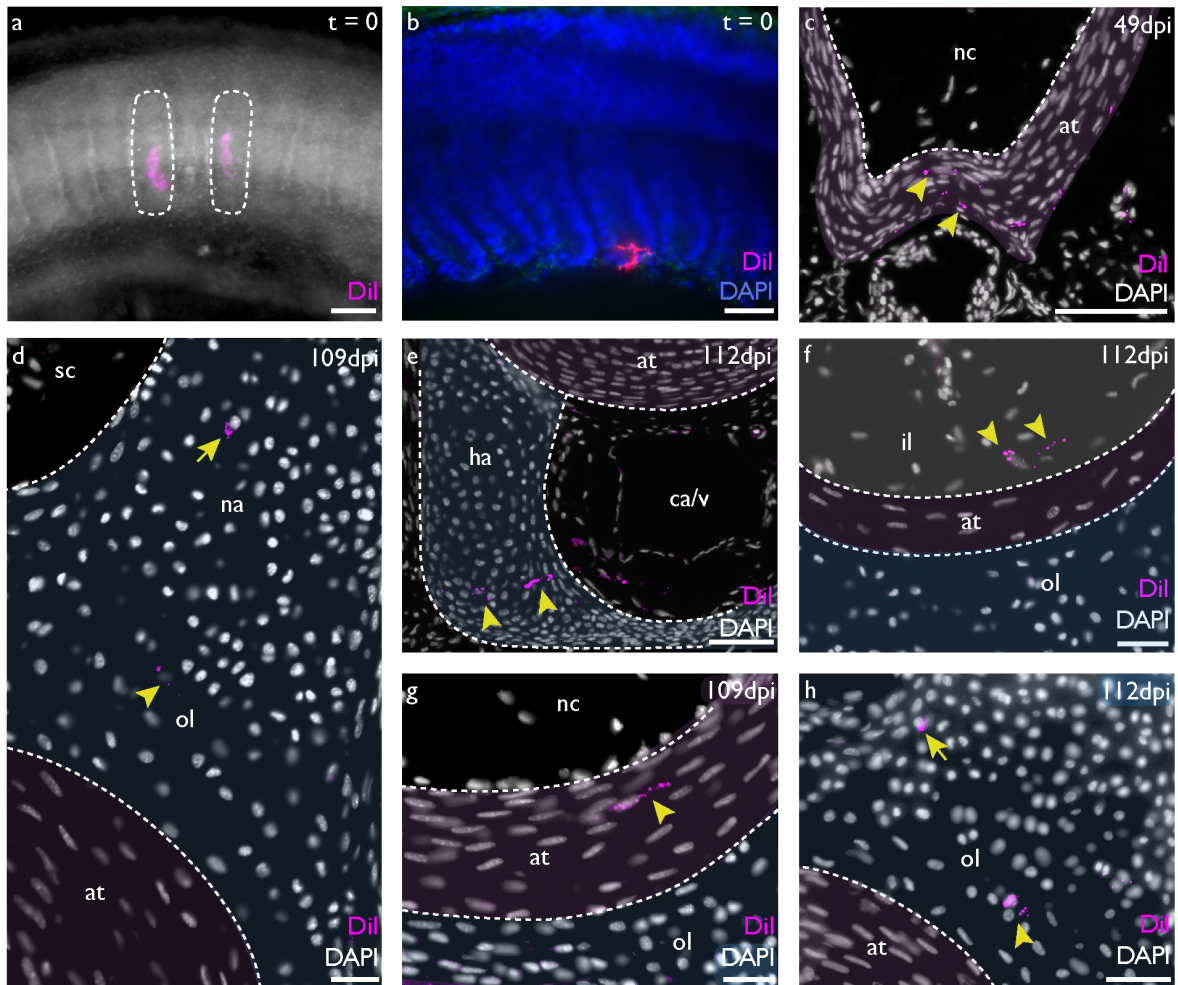
345 a', magnified cross section illustrating the three layers of the centrum; b, schematic

346 illustrating the components and tissues of the skate vertebra; b' schematic of the tri-layered
 347 centrum. at, areolar tissue; ce, centrum; ha, haemal arch; hsp, haemal spine; il, inner layer of
 348 the centrum; na, neural arch; nc, notochord; ne, notochord epithelium; nsp, neural spine; ol
 349 outer layer of the centrum; sc, spinal cord. Scale bar = 200 μ m.
 350



351
 352 **Figure 2. Microinjection of skate embryos with CM-DiI.** CM-DiI labeling of a, somites at
 353 S24 (three somites are highlighted with dashed lines) and b, notochord progenitor cells at S14
 354 (with the “notochord triangle” of Ballard et al. 1993 outlined). c, sealing of a windowed skate
 355 egg with donor egg shell. Scale bars = 200 μ m.

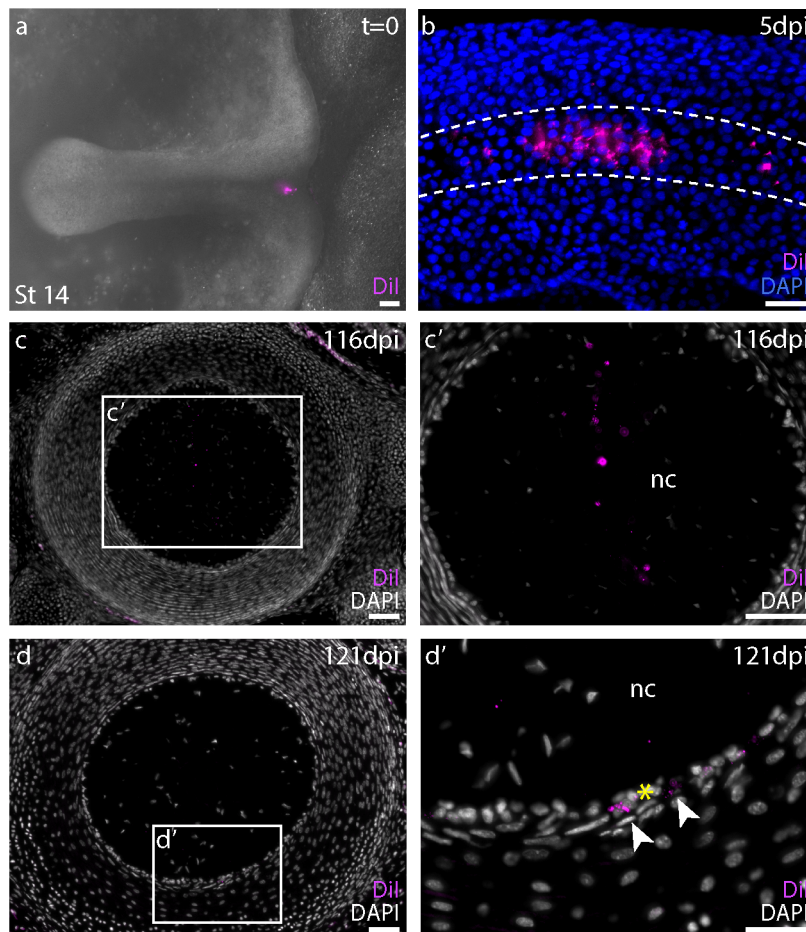
356



357

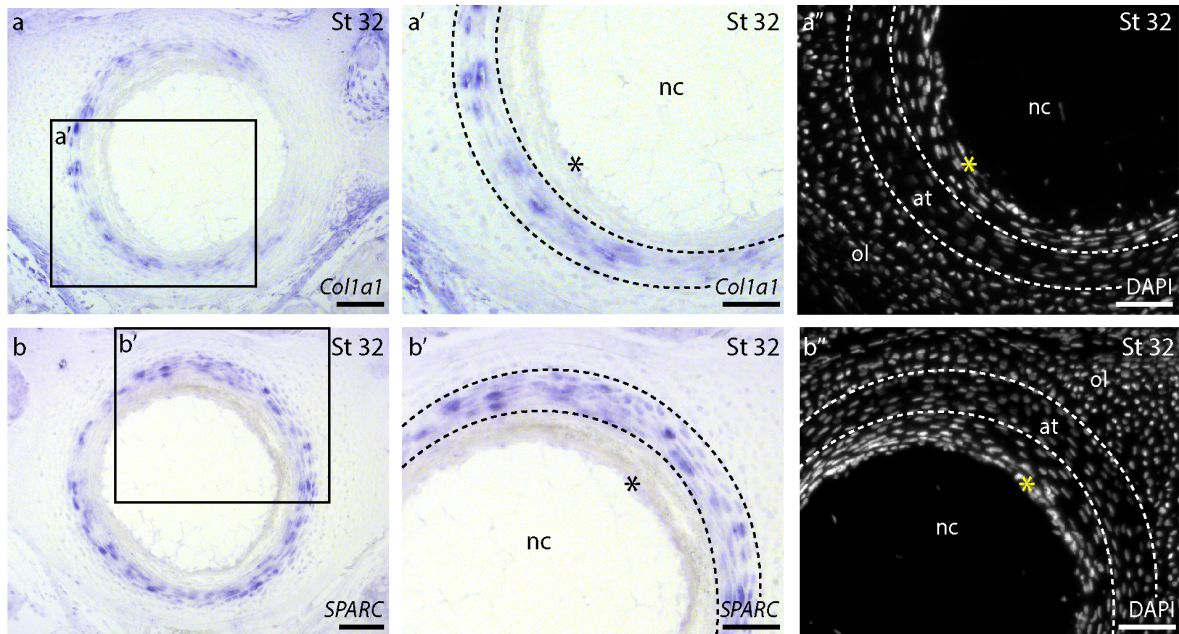
358 **Figure 3. Somitic contribution to the skate vertebral skeleton.** a, two CM-DiI injections in
 359 ventral somites; b, confocal image confirming the placement of the dye immediately post
 360 injection in sagittal section; c, CM-DiI labeled cells (indicated by yellow arrowheads)
 361 distributed within the spindle-shaped cells of the areolar tissue (at) at 49 dpi (false colored
 362 pink); d, CM-DiI labeled chondrocytes in the neural arch (na, indicated by yellow arrow) and
 363 outer layer of centrum cartilage (ol, indicated by yellow arrowhead) at 109dpi (cartilage false
 364 colored blue); e, CM-DiI labeled cells in the haemal arch at 112 dpi (ha, false colored blue);
 365 f, CM-DiI labeled chondrocytes (indicated by yellow arrowheads) in the inner layer of the
 366 centrum at 112 dpi (il, false colored white); g, CM-DiI labeled cells (indicated by yellow
 367 arrowhead) in the areolar tissue, the middle layer of the centrum at 109 dpi (at, false colored

368 pink); h, CM-DiI labeled chondrocytes in the outer layer of the centrum (ol, indicated by
 369 yellow arrowhead) and in the neural arch (indicated by yellow arrow) at 112 dpi (na, false
 370 colored blue). ca/v, caudal artery and vein; nc, notochord; sc, spinal cord. Scale bars = 100
 371 μm .
 372



373
 374 **Figure 4. No cellular contribution from the notochord to the skate vertebral skeleton.** a,
 375 CM-DiI injection of the notochord triangle of a skate embryo at S14; b, confocal image of a
 376 skate embryo at 5dpi, showing CM-DiI-labeled cell in the notochord; c, a section through the
 377 notochord at 116 dpi, showing CM-DiI positive notochord cells at 10x; c', higher
 378 magnification view of the inset box in c; d, CM-DiI positive cells in the notochord
 379 epithelium; d' higher magnification view of the inset box in d. Yellow asterisk indicates
 380 notochord epithelium. Scale bars = 100 μm .

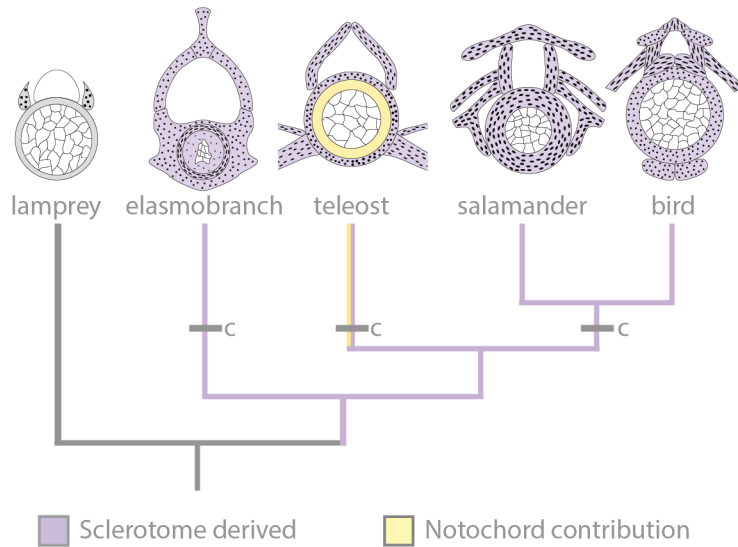
381



382

383 **Figure 5. The notochord is not a source of bone-like tissue in skate vertebral centra.** a,
 384 *Colla1* is expressed in the areolar tissue of the developing centrum; a', a higher-
 385 magnification image of *Colla1* expression; a'' DAPI staining of the same section as depicted
 386 in a', showing the boundary between areolar tissue and the notochord epithelium (yellow
 387 asterisk); b, *SPARC* is expressed in the areolar tissue of the developing centrum; b', a higher-
 388 magnification image of *SPARC* expression, and b'' DAPI staining of the same section as
 389 depicted in b', showing the boundary between areolar tissue and the notochord epithelium
 390 (yellow asterisk). at, areolar tissue; nc, notochord; ol, outer layer. Scale bars = 100 μ m.

391



392

393 **Figure 6. Embryonic origins of the vertebral skeleton across gnathostomes.**

394 Representative sections of lamprey, skate, teleost, salamander, and bird vertebrae, with
 395 paraxial mesodermal derivatives indicated by purple, and notochord derivatives indicated by
 396 yellow. Grey bars indicate independent originations of centra. Schematics redrawn after
 397 Goodrich [36] (lamprey), Criswell [15] (skate), and MacBride [37] (teleost, salamander, and
 398 bird).